DOI: https://doi.org/10.24297/jap.v17i.8718

Mathematical Modeling of Photovoltaic Properties of Nipc/P-Si (Organic/Inorganic) Heterojunction by Using Artificial Neural Networks Model

Mahmoud. Y. El-Bakry [1], R. A. Mohamed *[1], D. M. Habashy [1], E. H. Aamer [1]

[1]Theoretical Group, Physics Department, Faculty of Education, Ain Shams University, Cairo, Egypt

*rashaaam@yahoo.com

Abstract

In this research, the artificial neural network (ANN) and resilient back propagation (R-prop) training algorithm are utilized to model the photovoltaic properties of Nickel–phthalocyanine (NiPc/p-Si) heterojunction. The experimental data are extracted from experimental studies. Experimental data are utilized as inputs in the ANN model. Training of different structures of the ANN is processed to approach the minimum value of error. Eight artificial neural networks are trained to get a better mean square error (MSE) and best execution for the networks. The ANN performances are also investigated and their values are very small (MSE < 10^{-3}). The simulation results of the current-voltage characteristics of NiPc films are produced and provided excellent matching with the corresponding experimental data. Utilization of ANN model for predictions is also processed and gives accurate results. The equation which describes the relation between the inputs and outputs is obtained. The high accuracy of the ANN model has appeared in the major guessing power and the ability ofgeneralization depending on the obtained equations.

Keywords: Modeling – Artificial Neural Network (ANN) Model – Photovoltaic Properties - (Organic/Inorganic) Heterojunction.

Introduction

Organic semiconductors are hopeful candidates due to their role and diversity. Phthalocyannines are prototype organic semiconductors and are recognized by their high thermal and chemical stability. They form large groups of organic compounds which have been essential for the search because of their active properties for more than 40 years Linstead (1934). Organic semiconductors have many potential applications so that the researches on this field have been enlarged rapidly. Examples of these applications are the use of organic semiconductors in photovoltaic cells Wohrle and Meissner (1991), laser printers Gregory (1991), dyes, pigments, photocopying agents Haisch et. al. (1997), gas sensors Gardner et. al. (1992) and Mrwa et. al. (1995), optical data storage systems Ao et. al. (1995), solar cells Kerp and Faasen (2000), light emitting diodes Lee et. al. (1999), and also in nuclear reactor systems. In recent years an important jump of organic photovoltaic (PV) solar cells are achieved Reycroft and Ullai (1980), Ghosh et. al. (2001), Khelifi et. al. (1985), Mahapatro and Ghosh (2001), Tang (1986) and El-Nahass et. al. (2005).

Numerous studies have demonstrated the bio-inspired computing techniques such as artificial neural networks (ANNs) and evolutionary computing techniques can be alternative methods have long applied. ANNs are biologically inspired computer programs designed to simulate the way in which the human brain processes information El-Metwally et. al. (2000), Haweel et. al. (2003), El-Bakry (2003), (2004), Attia et. al. (2013) and Mohamed and Habashy (2018). Artificial neural network (ANN) model is proceeding quickly, and it is applied in different fields. It is an approach which imitates the human mental processes, where it holds computational power, ability of learning, generalization and prediction of acceptable outputs for the inputs that have not exist during a training step Nada et. al. (2013). Developments in ANNs and their applications to physics have made it feasible to model enormous characteristics in different areas in physics. Many investigations have been presented on utilizing ANN in modeling different properties of semiconductors. Darwish. et. al (2015) studied Optoelectronic performance and artificial neural networks (ANNs) modeling of n-InSe/p-Si solar cell. They found

CC BY

that the uses of an artificial neural network and R-prop training algorithm succeeded in predicting the optical constants of $As_{30}\ Se_{70-x}\ Sn_x$ (0≤x≤3). Ali and Mohamed (2018) utilized the artificial neural network in modeling the electrical impedance spectroscopy of (4E)-2-amino-3cyanobenzo[b]oxocin-6-one. They found that ANN simulated the experimental data with a very high accuracy and predicted new values that were unmeasured experimentally. Also, they showed that artificial neural network model is a very effective tool in modeling and able to follow the patterns of the experimental data with a high precision. El-Barry and Habashy (2019) studied the Optical characterization of casting (Adamantan Fulgide) thin films using (CTANNs) approach. They found that modeling of optical characterizations of casting (Admantan-Fulgide) thin films with different concentrations by using ANN provided accurate results and low error rates. El-Barry and Mohamed (2019) studied of photovoltaic characteristics of pyronine thin film/p-Si single crystal experimentally and theoretically by using ANN model. They found that the ANN trained results are in excellent matching with the experimental data and the generalization process provided accurate predicted results. Mohamed (2019) utilities ANN model to predict of alternating current (AC) conductivity for different samples of organic semiconductors. He found that using of ANN model is considered a very successful tool to predict the AC conductivity for organic semiconductors. Also he concluded a generalized equation to predict AC conductivity for any other organic semiconductor.

In this paper, ANN is used to model the photovoltaic properties of NiPc/p-Si (organic/inorganic) heterojunction. We will try to use ANN model to simulate the experimental data, predict values are in the experimental data range as a testing step, make predictions for values are not exist in the experimental data range as an application for the generalization process and finally we will introduce the equation which describes the physical behavior under study. In this respect, the paper organized in five sections, the first section gives a brief introduction and showed some important researches from literatures, the second displays the experimental procedures, the third introduces brief notes on ANN model, the fourth discusses the results, the last section displays our conclusions.

Experimental data

The NiPc powder utilized in this study is acquired from Kodak, UK. pieces of p-silicon of 1 cm^2 each and 450 µm thick were scrubbed and treated with etching solution of CP4 (HF: HNO_3:CH_3COOH in ratio 1:6:1). After etching, the Si wafers were solved in distilled water and then with ethyl alcohol. After the Si-substrate cleaning and etching, Nipc thin film with different thicknesses were deposited on the front side of the substrate by conventional thermal evaporation technique, and then the NiPc layer was covered by an Au mesh to be applied as an ohmic electrode. The back side of Si was coated by a thick layer of aluminum electrode. The fabricated NiPC/P-Si heterojunction was annealed at 373 for 2 hours to enhancement the performance of heterojunction under investigation. Measurements of dark current-voltage characteristics within the temperature range 298-373 K were produced in air. A stabilized power supply and a Keithley were used to determine the current abundance through the cell by 617 an electrometer. Mean of Pt-PtRh thermocouple with monitor (philips thermostat PT 2282 A) was utilized to determine the temperature directly. A proportional temperature controller (Euro-therm. model no. 390-200) was hired to shun the sudden drop in the heater temperature. the cells illuminated by light coming from a light source (white light) with an intensity for incident power of 6 mW/cm^2. The dark C-V characteristics were determined at 1 MHz using Model 410 CV Meter El-Nahass et. al. (2005).

Artificial neural network model

Artificial neural network contains of simple processing units which operate by transmitting signals to each other over a huge number of weighted connections. Neurons are the "building blocks" of neural networks as units or nodes. Basically, inputs are received from many other neurons counting on the processing function of the neuron, the current input is used to change its internal state (activation), sends one output signal to many other neurons. Forward networks supply the most popular neural network. During the training process, the network detects its weights and bias to reach to the least error and the best performance of networks. In this research, resilient back-propagation algorithm (R-prop.) is the training algorithm used in artificial neural networks model.

R-prop is utilized to eliminate the failed effects during training. These effects caused by the values of partial derivatives that yield from applying the transfer functions (the sigmoid functions) to the outputs. Fig 1 introduces

CC BY

a Simple neuron model. It consists of inputs, the activation function and output. Each input X_n is weighted by a factor W_n. The sum of all inputs is calculated. Then an activation function f is applied to the resultant to produce the neural output $f_{(a)}$. As shown in the following equations:

The sum of weighted inputs = $(\sum_{allinputs} W_n X_n)$

$f_{(a)} = activationfunction\ (\sum_{allinputs} W_n X_n)$

Where n is the number of inputs. Mohamed (2019).

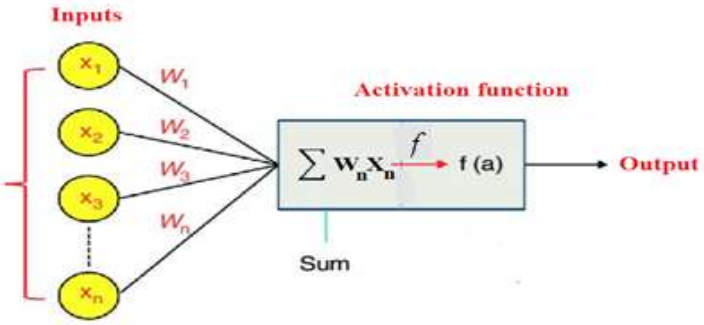

Figure 1a Simple neuron model

In this research, the artificial multilayer neural network is utilized for modelling the experimental data. It consists of three types of layers. The first type of layers; the input layer contains the inputs. While the second type of layers is the hidden layers where the neurons organized. The last type of layers includes the neuron output called output layer. Figure1b demonstrates a schematic presentation of an artificial multilayer neural network structure. The network follows the supervised learning rule. During the training process, the network iteratively adjusts connection weights and biases until the network results simulate the targets with high precision. In this approach, backpropagation error adjustment (BPE) is the utilized modification technique.

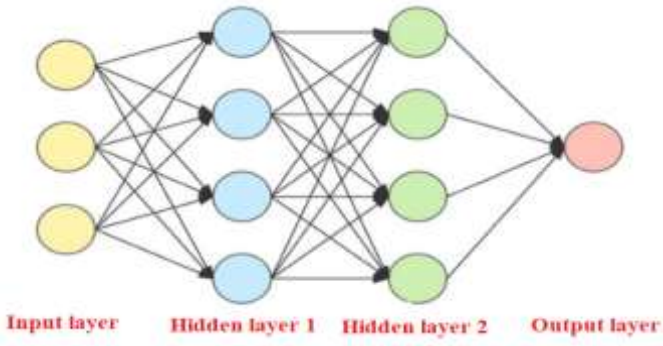

Figure 1b. Schematic diagram for the artificial multilayer neural network

The ANN performances calculated using the mean squared error (MSE) for the training dataset. It can be calculated using the following equation.

$$MSE = \sqrt{\frac{1}{n}\sum_{i=1}^{n}(y_{pred.} - y_{exp.})^2}$$

CC BY

Where $y_{exp.}$is the experimental data, $y_{pred.}$ is the ANN predicted results, $\overline{y}$ is the average and n is number of inputs.

Results and discussion

a- Dark current –voltage characteristics

Eight individual neural networks are trained separately to model the experimental data. Table 1. Summarizes the main features of the eight networks. It includes the number of hidden layers (HLS), the number of nodes (ANs), inputs, the number of epochs, the best (MSE) performance and outputs for modelling of the photovoltaic characteristic of NiPc/p-Si heterojunction.

Table 1 Modelling overview of photovoltaic characteristic of NiPc/p-Si heterojunction.

The trained ANN	HLs	ANs	Inputs	epochs	Start	The best (MSE)	Outputs
Net. 1	3	10,30,40	2 (V,T)	500	120.79	0.00034354	I
Net. 2	3	300,400,500	1(V)	988	8.46 x 10^{12}	2.4781 x 10^{-21}	R_j
Net. 3	3	800,400,800	2 (V,T)	961	3.5 x 10^{5}	4.853 x 10^{-13}	I_f
Net. 4	3	100,40,30	2 (logV, T)	500	582941.5	6.0149 x 10^{-9}	Log I
Net. 5	3	800,750,800	2 (V,T)	1219	3.906 x 10^{5}	9.7026 x 10^{-15}	I_R
Net. 6	3	10,20,5	1 (V)	307	33.16	2.2087 x 10^{-8}	C^2
Net. 7	3	100,40,30	1 (V)	90	2771.7	1.0784 x 10^{-11}	W^2
Net. 8	3	100,200,150	1 (V)	308	121981.6	6.263 x 10^{-13}	I

First neural network was trained using experimental data current-voltage characteristics of NiPc/p-Si (organic/inorganic) heterojunctions. It contains two inputs voltage (V) and temperature (T) and one output current (I) as shown in Fig. 2 and table 1.

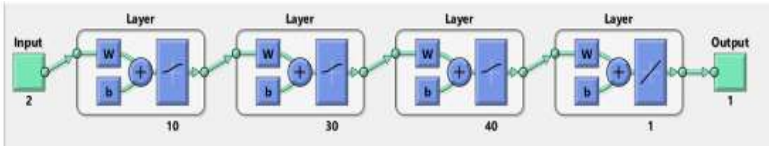

Figure 2. construction of 1st ANN

Figure 3a. shows the training procedure which reveals that the mean squared error of the network starting at a large value and diminishing to reach the best (MSE) performance value at 0.0034345 after 500 epochs. The number of epochs represent the number of neural network iterations. It is clear from the performance curve that it Starts with a large value of (MSE) then by iterations the (MSE) reaches to a very small value that confirms a successful ANN learning process. Figure 3 b. shows the current-voltage characteristics simulation results of NiPc films together with the corresponding experimental data for temperature range 298-373 K and the predicted results for 273, 298 and 340 K. It is clearly observed that ANN gives high precision results.

CC BY

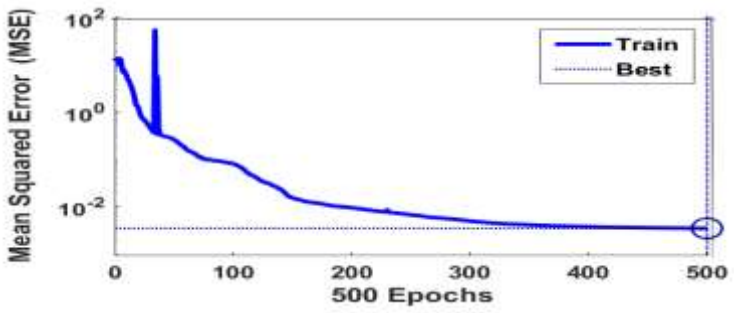

Figure 3a. performance of ANN for current-voltage characteristics of NiPc films

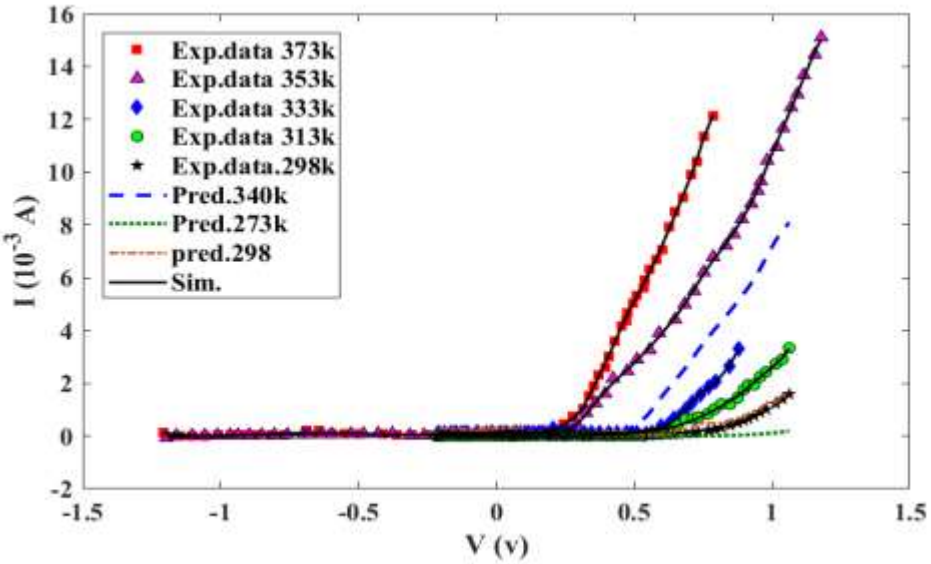

Figure 3b. Comparison between the trained ANN results and the experimental data for dark current-voltage characteristics NiPc/p-Si films at different temperatures

The Second artificial neural network contains one input (the junction resistance) and one output (the voltage) as shown in Table 1. figure 4. shows schematic diagram for the construction of the second artificial neural network. Figure 5a. shows the training procedure which reveals that the best mean squared error value 2.4781 $\times 10^{-21}$ at 988 epochs. Figure 5b. shows the ANN simulation results for junction resistance R_j ,versus V for NiPc /p-Si together with the corresponding experimental data. It is clearly observed that The ANN results and the experimental data are in good agreement. The third artificial neural network contains two inputs (the voltage and the temperature) and one output (the current) as shown in Table 1. figure 6. demonstrates the construction of the third artificial neural network.

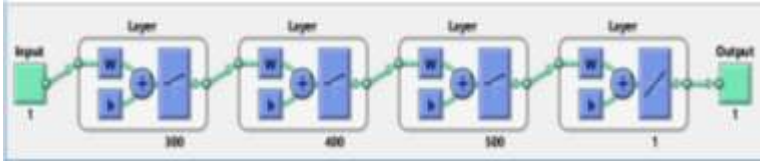

. Figure 4. construction of the 2nd ANN

CC BY

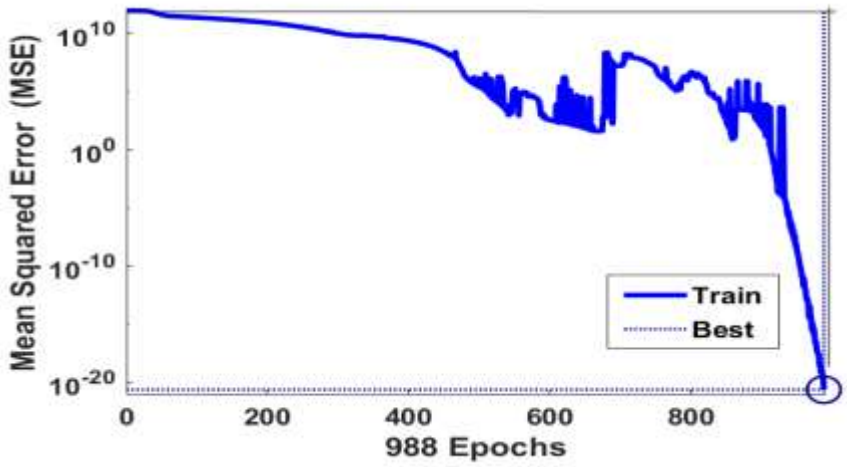

Figure 5a. The performance of 2nd ANN

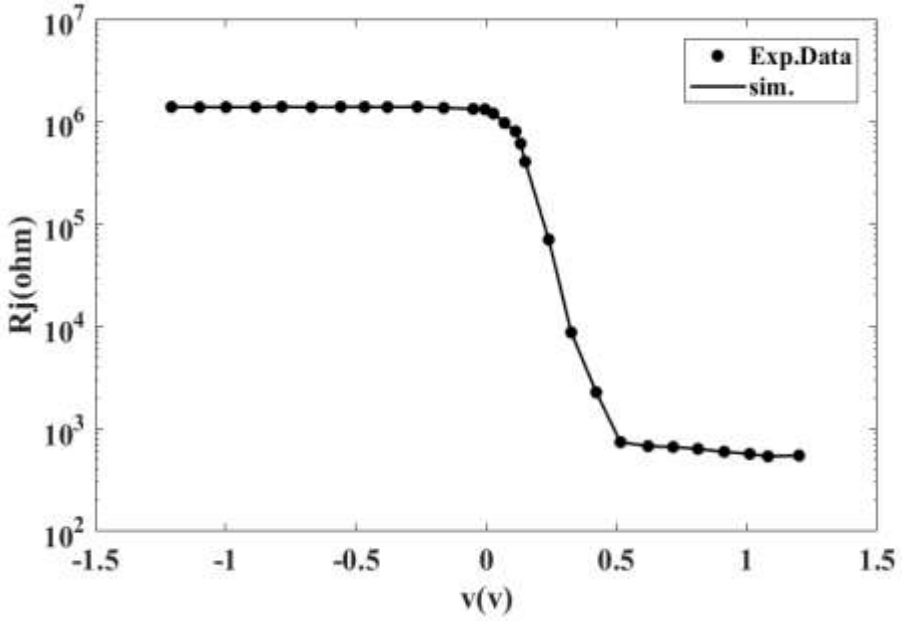

Figure 5b. The simulation results of the junction resistance R_j using ANN model

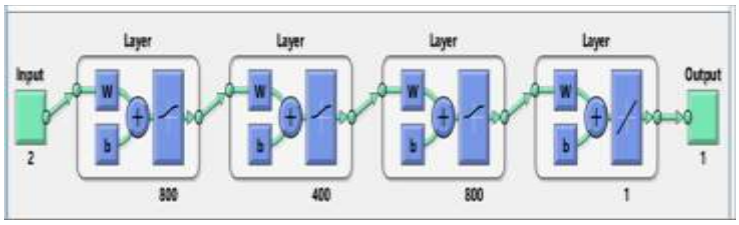

Figure 6. The construction 3rd ANN

Figure 7a. shows the training performance which reveals that the mean squared error of the network starting at a large value and diminishing to reach a best value of 4.853×10^{-13} after 961 epochs. Figure 7b. shows the simulation results of the current-voltage characteristics of NiPc films together with the corresponding experimental data for temperature range 298-373 K.

CC BY

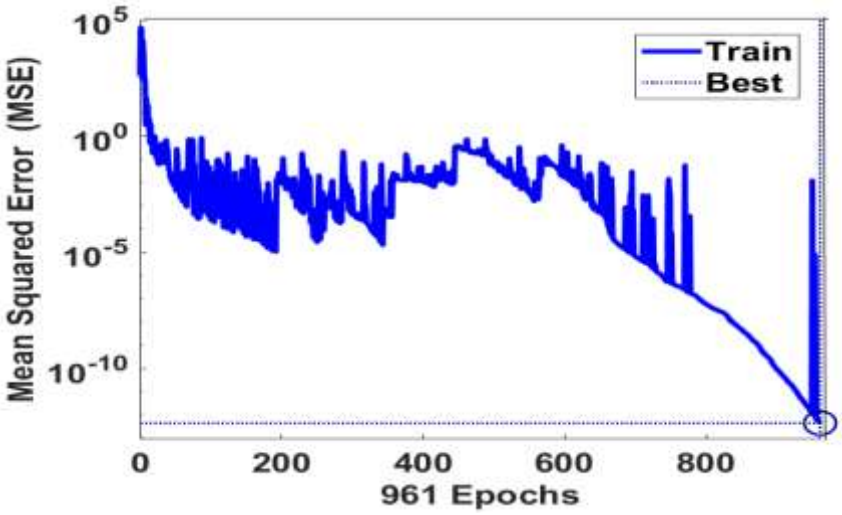

Figure 7a. The performance of 4th ANN

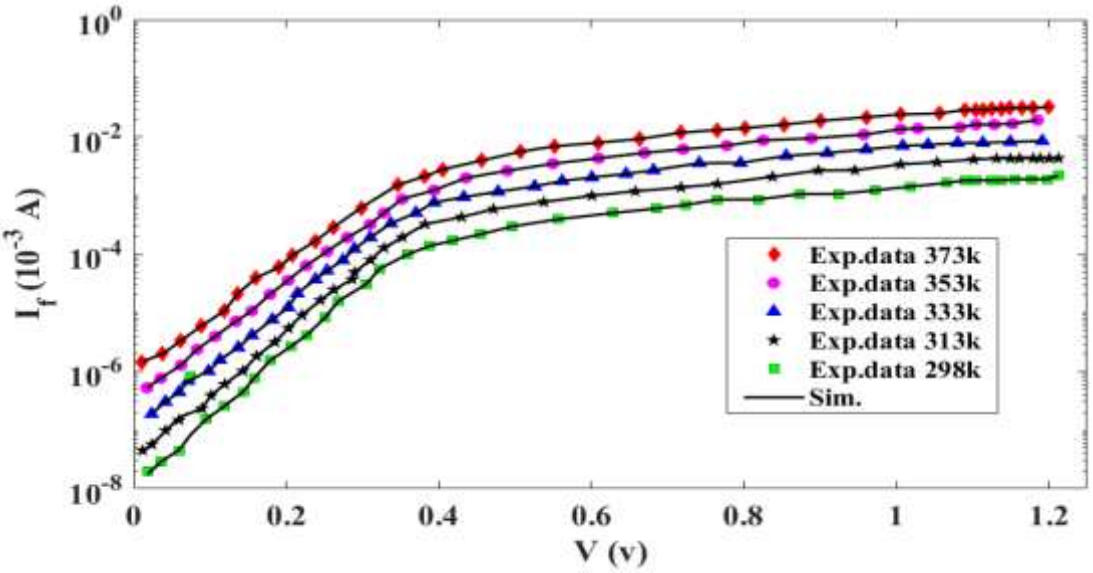

Figure 7b. ANN simulation results for the semi-logarithmic plots of forward current–voltage characteristics of NiPc/p-Si heterojunction at various temperatures

The fourth artificial neural network contains two inputs (log v and temperature) and one output (log *I*) as shown in Table 1 and Fig. 8.

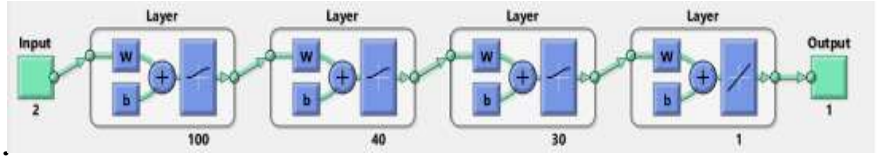

Figure 8. The construction of 4th ANN

CC BY

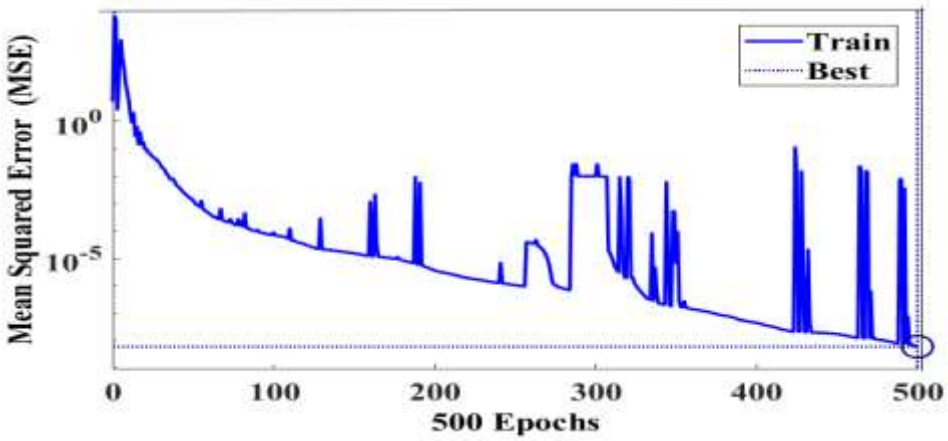

Figure 9a. The performance of 4th ANN

Figure 9a shows the training performance and the mean squared error for the forth network starting at a large value and diminishing to reach a best value of 6.0149 x 10^{-9}after 500 epochs. Figure.9b shows the ANN simulation results of the current-voltage characteristics of NiPc films together with the corresponding experimental data for temperature range 298-373 K and the predicted current at 273, 373, 360 and 380 K. It is clearly observed that ANN trained results is very precise.

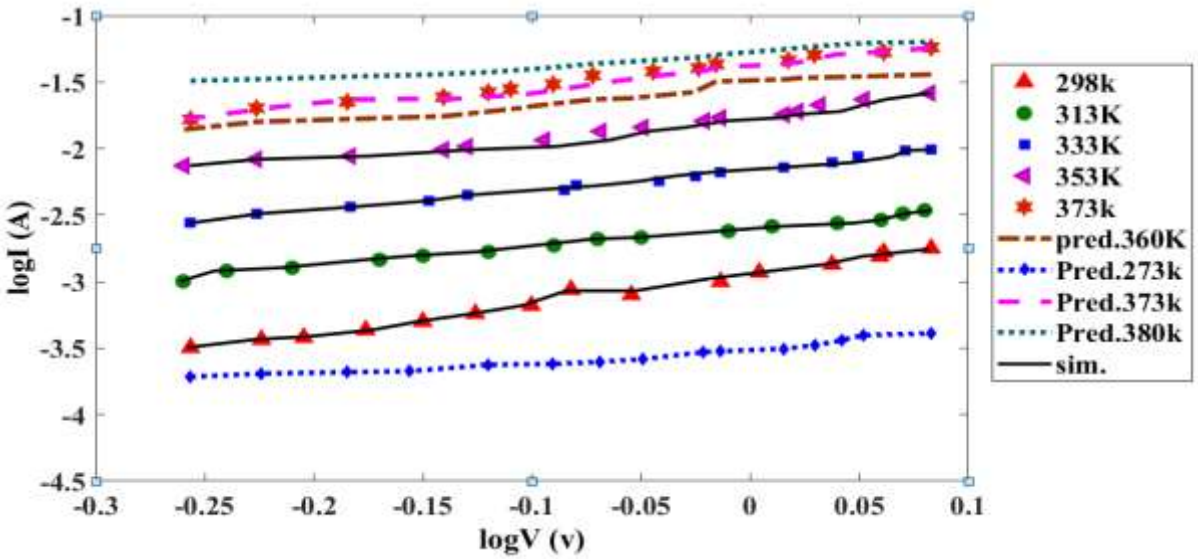

Figure 9b. The trained ANN results (simulated and predicted) for variation of log *I* with log *V* at higher forward voltage bias for NiPc/p-Si heterojunction at different temperatures

The fifth artificial neural network contains two inputs (voltage and temperature) and one output reverse current) as shown in Table and Fig.10.

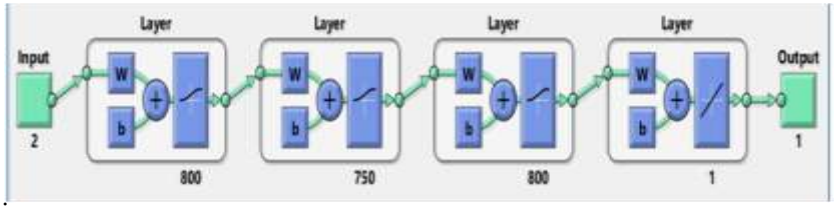

Figure 10. The Construction of 5th ANN

CC BY

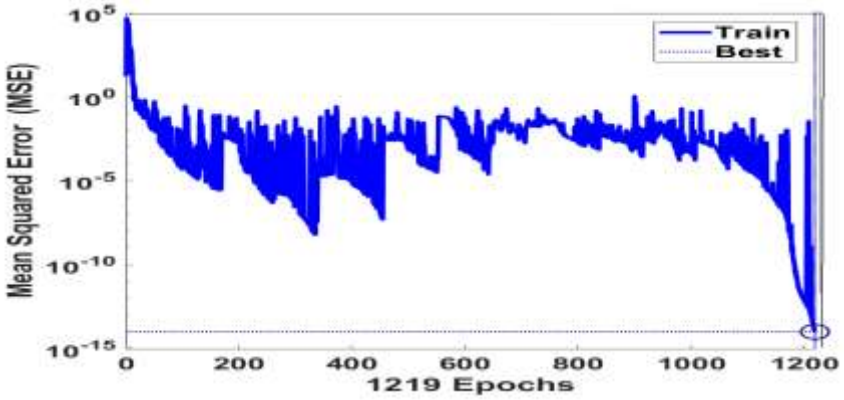

Figure 11a. The performance of 5th ANN

Figure 11a. shows the MSE for the fifth neural network. The best MSE is equal to 9.7026×10^{-15} at 1219 epochs. Figure 11b. shows the simulation results of semi-logarithmic plots of the reverse bias of *I-V* characteristics of NiPc films together with the corresponding experimental data for temperature range 298-373 K. It is clearly observed that the trained ANN results and the experimental data are in good agreement.

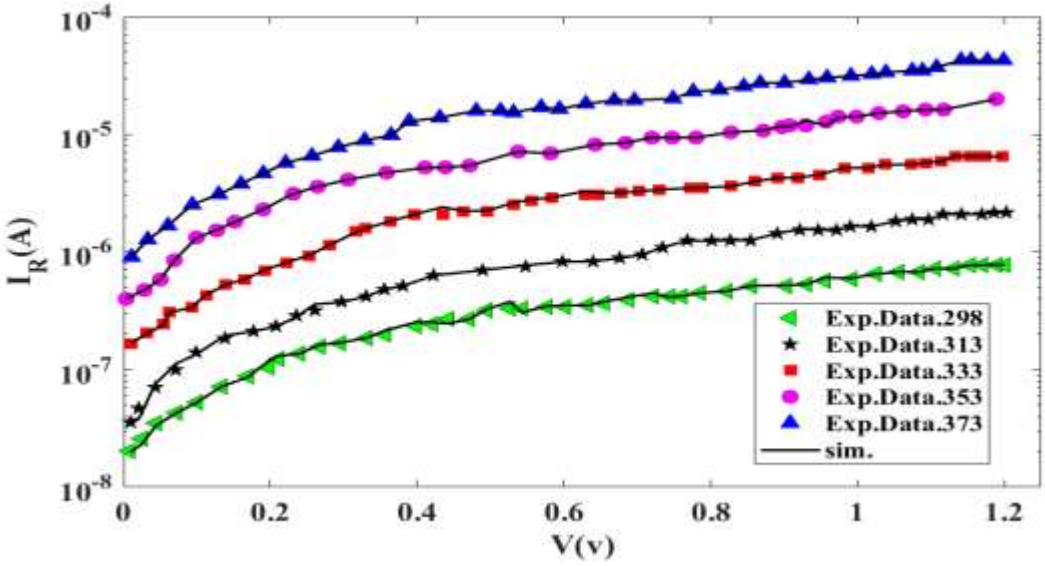

Figure 11 b. comparison between ANN simulation results and the experimental data for a semi-logarithmic plot of the reverse bias of *I-V* characteristics for NiPc/p-Si heterojunction at different temperatures

B-Dark current –capacitance characteristics

The sixth artificial neural network contains one input (voltage) and one output (C^{-2}) as shown in table 1. The construction of the sixth network are shown in Fig. 12. Figure 12. represents the number of hidden layers, number of neurons in each hidden layer and the activation functions for the 6th network.

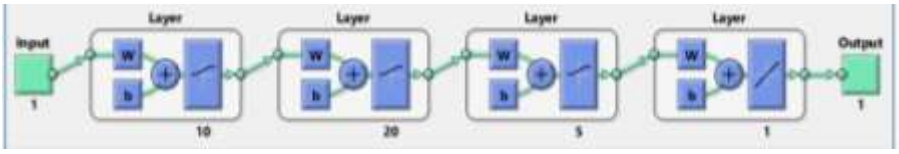

Figure 12. The construction of the 6th ANN.

CC BY

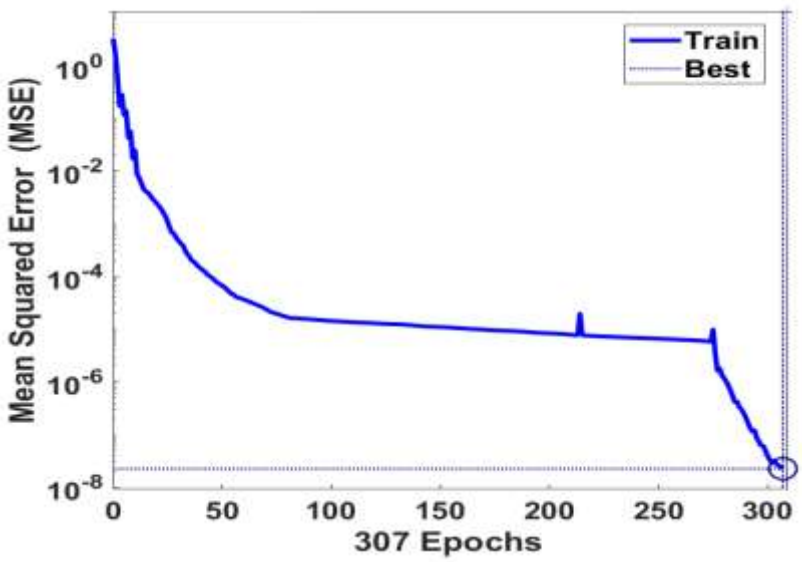

Figure 13a. The ANN performance for the 6th network

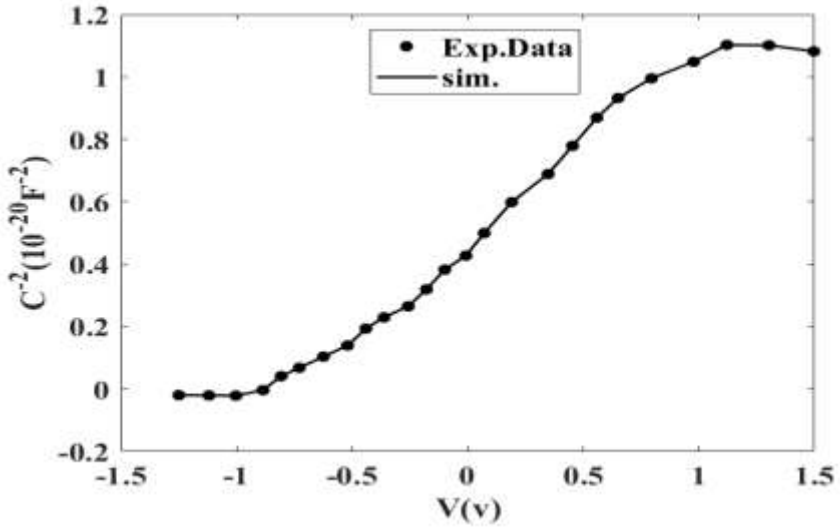

Figure 13 b. The ANN results and the experimental data C^{-2}-V characteristics for NiPc/p-Si heterojunction.

Figure.13a. shows the ANN performance and the best mean squared error for the sixth network that equal to 2.2087×10^{-8} at 307 epochs. Figure 13 b. shows the ANN simulation results for C^{-2}-V characteristics of NiPc films together with the corresponding experimental. It is clearly observed that ANN simulated curve completely coincides with the experimental data points and that introduces excellent performance for the ANN model. The seventh artificial neural network contains one input (voltage) and one output (width of the depletion region) as shown in Table 1.

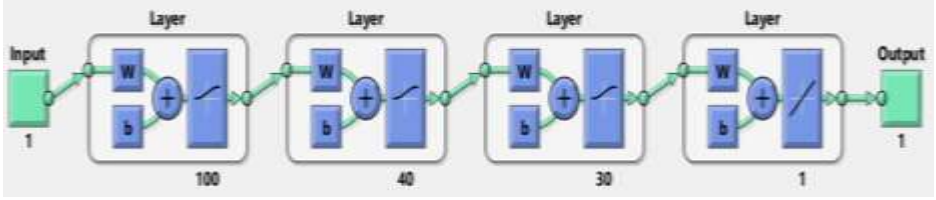

Figure14. The construction of the seventh artificial neural network

CC BY

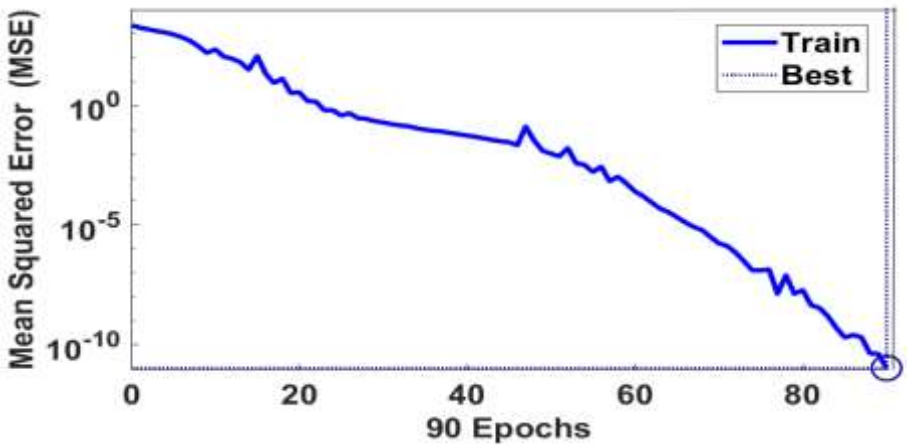

Figure 15a. The ANN performance for the W^2-V characteristics of NiPc/p-Si heterojunction.

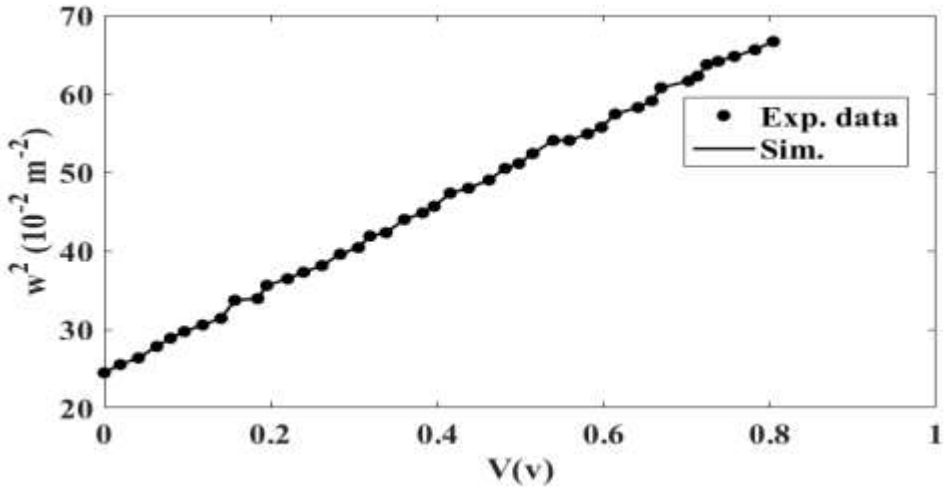

Figure 15b. Relation between width of the depletion region and voltage with the corresponding ANN simulated results.

Figure15a shows the ANN performance for the seventh network and the mean squared error starting at a large value and diminishing to reach a best value at 1.0784×10^{-11} after 90 epochs. The best MSE confirms that the learning process is carried out successfully. Figure 15b shows the ANN simulation results for the W^2-V characteristics of of NiPc films together with the corresponding experimental. The eighth artificial neural network contains one input (voltage) and one output (current for illumination and dark) as shown in Table 1. Figure 16 shows the construction for the eighth network.

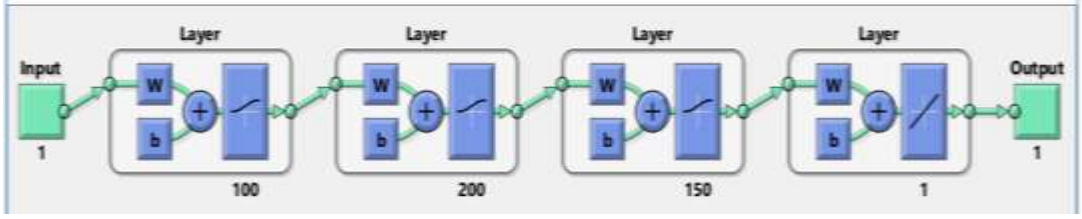

Figure16 The construction of the 8th ANN

CC BY

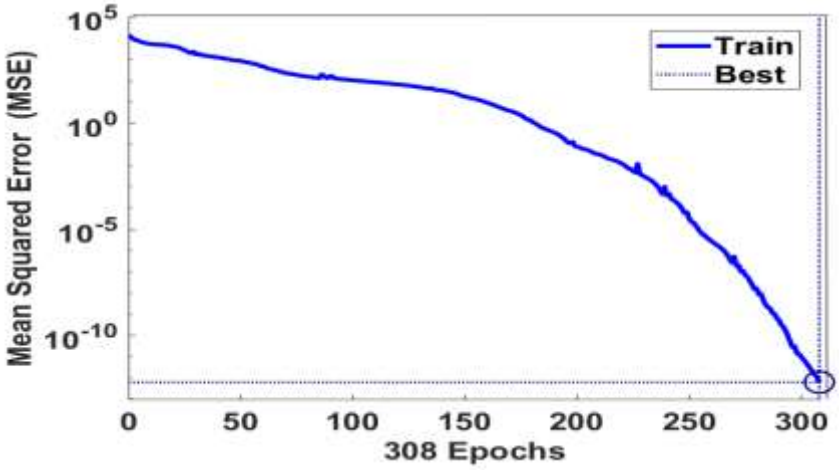

Figure 17a The performance of ANN model $I-V$ characteristics under illumination and dark for NiPc/p-Si films.

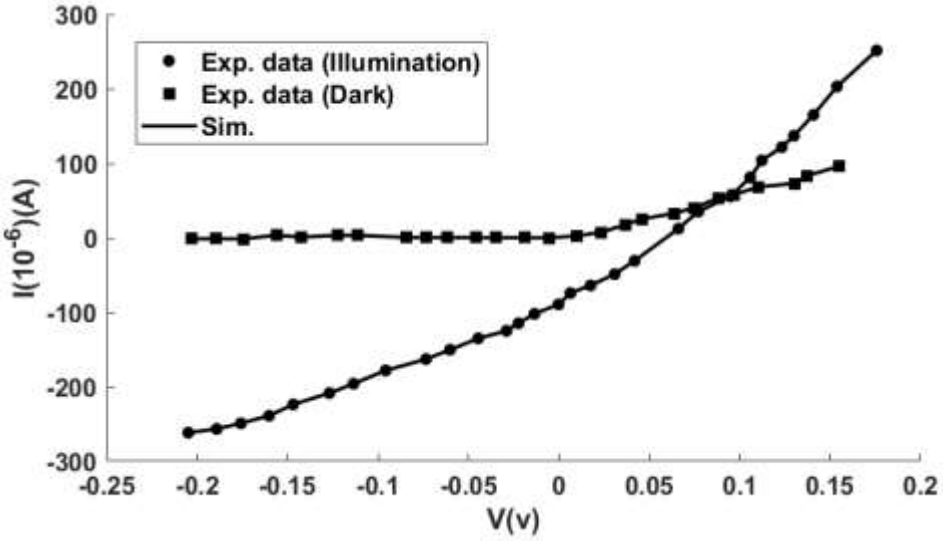

Figure 17b the experimental data and ANN simulation results for the current –voltage characteristics under illumination and dark for NiPc/p-Si heterojunction.

Figure 17a introduces the performance containing the learning curve and the best value using the mean squared error function. The best MSE is 6.2653×10^{-13} at 308 epochs. Figure17b represents the ANN simulation results for $I-V$ characteristics under illumination and dark for NiPc films together with the experimental data. It is clearly observed that the trained ANN results and the measured curves (experimental data) are in good agreement. The equation which describes the physical behavior of the photovoltaic properties of NiPc/p-Si heterojunction is given in Appendix A.

Conclusion

In this research, ANN model used to model the photovoltaic properties of NiPc/p-Si (organic/inorganic) heterojunction. The experimental data extracted from previous practical studies. These data used as inputs in the ANN model. The model has been trained in different topologies in order to obtain the best neural network structure providing the least error. Eight neural networks were trained to model the experimental data their constructions introduced in the discussion. They consist of three hidden layers containing different numbers of neurons in each layer. The R-Prop train function (trainrp) and log-sigmoid (logsig) utilized as the training

CC BY

algorithm and transfer function, respectively. The best performance achieved for all networks did not exceed 10^3 by using the mean squared error MSE function. The ANN predicted results at values of 298 K for dark current–voltage characteristics and 373 K for variation of log *I* with log *V* of NiPc/p-Si heterojunction which measured experimentally introduce an excellent accordance with the experimental data. Also, the predicted ANN results at 273 and 340 K for dark current–voltage characteristics and at 273 ,360 and 380 K for variation of log *I* with log *V* of NiPc/p-Si heterojunction which are not measured. The most important result presented in the research is the mathematical relation which describes the behavior of the photovoltaic properties of NiPc/p-Si (organic/inorganic) heterojunction. It is clear from the trained results that the ANN model was able to follow the target patterns very efficiently and was even able to predict values which had not been measured in practice. Therefore, ANN can be considered a powerful tool for estimating photovoltaic properties of NiPc/p-Si (organic/inorganic) heterojunction.

References

1. Ao, R., Kümmerl, L., Haarer, D. (1995). Present limits of data storage using dye molecules in solid matrices, Adv. Mater., 7 495-499. https://doi.org/10.1002/adma.19950070522

2. Ali, H. A. M., Mohamed R. A. (2018). Modeling for electrical impedance spectroscopy of (4E)-2-amino-3cyanobenzo[b]oxocin-6-one by artificial neural network, Ceramics International, 44 10907-10911. https://www.sciencedirect.com/science/article/pii/S0272884218307107?via%3Dihub

3. Attia, A.A., El-Nahas, M.M., El-Bakry, M.Y., Habashy, D.M. (2013). Neural networks modeling for refractive indices of semiconductors, Opt. Commun. 287 140-144. https://doi.org/10.1016/j.optcom.2012.09.016

4. Darwish, A.A.A. Hanaf$y$, T.A., Atti$a$, A. A., Habash$y$, D.M., El-Bakr$y$, M.Y., El-Nahas, M. M., (2015). Optoelectronic performance and artificial neural networks (ANNs) modeling of n-InSe/p-Si solar cell, Superlattices and Microstructures 83 299-309. https://doi.org/10.1016/j.spmi.2015.03.033

5. El-Bakry, M.Y. (2003). Feed forward neural networks modeling for K–P interactions, Chaos Soliton Fract, 18 995-1000. https://doi.org/10.1016/S0960-0779(03)00068-7

6. El-Bakry, M.Y. (2004). A STUDY OF K–P INTERACTION AT HIGH ENERGY USING ADAPTIVE FUZZY INFERENCE SYSTEM INTERACTIONS, Int. J. Mod. Phys. C, 15 1013-1020. https://doi.org/10.1142/S0129183104006467

7. El.Barry, A.M.A., Habashy, D.M., (2019). Simulation and prediction of optical characterization of casting (Adamantan Fulgide) thin films using (CTANNs) approach.33(11) 1950093 https://doi.org/10.1142/S0217979219500930

8. El-Barry, A.M.A., Mohamed, R. A., (2019). Modeling of photovoltaic characteristics of pyronine thin film/p-Si single crystal, Material Research Express, 6(7) 2053-1591. https://doi.org/10.1088/2053-1591/ab0a34

9. El-Metwally, K.A., Haweel, T.I., El-Bakry, M.Y. (2000). A universal neural network representation for hadron hadron interactions at high-energy, Int. J. Mod. Phys. C, 11 619 - 629. https://doi.org/10.1016/S0129-1831(00)00053-5

10. El-Nahass, M.M., Farag, A.A.M., Darwish, A.A.A. (2005). Photovoltaic properties of NiPc/p-Si(organic/inorganic) heterojunctions, Organic Electronics, 6 129-136. https://doi.org/10.1016/j.orgel.2005.03.007

11. Gardner, J.W., Iskandari, M.Z., Bott, B. (1992). Effect of electrode geometry on gas sensitivity of lead phthalocyanine thin films, Sensors Actuators B 9 (2) 133 - 142. https://doi.org/10.1016/0925-4005(92)80206-D

12. Ghosh, A.K., Morel, D.L., Feug, T., Shaw,R. F., Rowe, C. (1974). Photovoltaic and rectification properties of Al/Mg phthalocyanine/Ag Schottky-barrier cells, J. Appl. Phys. 45 230. https://doi.org/10.1063/1.1662965

13. Gregory, P. (1991). High-technology Applications of organic colorants, plenum press, New York https://doi.org/10.1007/978-1-4615-3822-6

14. Haisch, P., Winter, G., Hanack, M., Lüer, L., Egelhaai, H., Oelkrug, D. (1997). Soluble alkyl- and alkoxy-substituted titaniumoxo phthalocyanines: Synthesis and photoconductivity, advanced materials, 9 (4) 316-321. https://onlinelibrary.wiley.com/toc/15214095/1997/9/4

15. Haweel, T.I. El-Bakry, M.Y., El-Metwally, K. A. (2003). Hadron–hadron interactions at high energy via Rademacher functions, Chaos Solitons Fract., 18 (2003) 159 168. https://www.sciencedirect.com/science/article/abs/pii/S0960077902005817

16. Kerp, H.R., van Faasen, E.E. (2000). Effects of oxygen on exciton transport in zinc phthalocyanine layers, Chem. Phys. Lett. 5 5-12. https://doi.org/10.1016/S0009-2614(00)01227-6

17. Khelifi, M., Mejatty, M., Berrchar, J., Bouchrriha, H. (1985). Photovoltaic effect in thin layers of phthalocyanines, Rev. Phys. Appl. 20 511-521. https://doi.org/10.1051/rphysap:01985002007051100

18. Lee, S.T., Wang, Y.M., HOU, X.Y., Tang, C.W. (1999). Interfacial electronic structures in an organic light-emitting diode, Appl. Phys. Lett., 74 (5) 670-672. https://doi.org/10.1063/1.122982

19. Linstead, R.P. (1934). Phthalocyanines. Part I. A new type of synthetic coloring matters, Journal of the Chemical Society, Part I 1016. https://doi.org/10.1039/JR9340001016

20. Mahapatro, A.K., Ghosh, S. (2001). High rectification in metal-phthalocyanine based single layer devices, IEEE Trans. Electron 48 (9) 1911-1914. https://doi.org/10.1109/16.944176

21. Mohamed, R. A., Habashy, D. M. (2018). Thermal Conductivity Modeling of Propylene Glycol - Based Nanofluid Using Artificial Neural Network, Journal of advances in physics, 14 (1) 5281-5291. https://rajpub.com/index.php/jap/article/view/7177

22. Mohamed, R. A. (2019). Prediction of AC conductivity for organic semiconductors based on artificial neural network ANN model, Material Research Express, 6(8) 085107-14 pages. https://doi.org/10.1088/2053-1591/ab250a

23. Mrwa', A., Friedrich', M., Hofmann, A., Zahn, D.R.T. (1995). Response of lead phthalocyanine to high NO_2 concentration, Sensors Actuators 25 596 - 599. https://doi.org/10.1016/0925-4005(95)85130-5

24. Nada, R.H., Habashy, D.M., AbdEl-Salam, F., El-Bakry, M. Y., Abd El-Khalek, A.M., Abd E;-Reheim, E. (2013). Modeling of aging process for supersaturated solution treated of Al–3wt%Mg alloy, Mater. Sci. Eng. A 567 80-83. https://doi.org/10.1016/j.msea.2013.01.009

25. Reycroft, P.J., Ullai, H. (1980). Photovoltaic properties of polymer films, Solar Energy Mater. 2 217-228. https://doi.org/10.1016/0165-1633(79)90019-4

26. Tang, C.W. (1986). Two-layer organic photovoltaic cell, Appl. Phys. Lett. 48 183-185. https://doi.org/10.1063/1.96937

27. Wohrle, D., Meissner, D. (1991). Organic solar cells, Adv. Mater. 3 129 - 138. https://doi.org/10.1002/adma.19910030303

CC BY

Appendix

The equation which represents the relation between inputs and outputs for all networks of NiPc/p-Si heterojunction by

$$a = Pureline\left[net.Iw\{4,3\}\frac{1}{1+e^{-n}}\left(net.lw\{3,2\}\frac{1}{1+e^{-n}}\left(net.lw\{2,1\}\frac{1}{1+e^{-n}}(net.Iw\{1,1\}n + net.b\{1\})\right.\right.\right.$$
$$\left.\left.\left. + net.b\{2\}\right) + net.b\{3\}\right) + net.b\{4\}\right]$$

Where n is input, a is output, net. lw{1,1};linked weights between the input layer and the first hidden layer, net.lw{2,1};linked weights between the first hidden layer and the second hidden layer, net.lw{3,2};linked weights between the second hidden layer and the third hidden layer, net.lw{4,3};linked weights between the third hidden layer and the output layer, net.b{1} is the bias of the first hidden layer, net.b{2} is the bias of the second hidden layer, net.b{3} is the bias of the third hidden layer and net.b{4} is the bias of the output layer

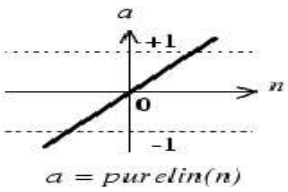

$a = purelin(n)$

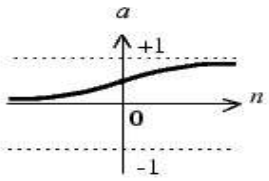

$a = logsig(n)$

Prof. Dr. Mahmoud Yasseen El-Bakry was born in Egypt 1958. Prof. Dr. Mahmoud is a researcher in Theoretical Physics and Artificial intelligence. Prof. Dr. Mahmoud received the B. Sc. (1981), M.Sc. (1987) and Ph.D. (1994) degrees in Theoretical Physics from Faculty of Science, Ain Shams University. Prof. Dr. Mahmoud is a professor and the head of physics department during the period (2015-2018) in Faculty of Education, Ain Shams University. His main interests in research are Artificial Intelligence (Neural Networks - Genetic programming – Neuro Fuzzy) and its application in Physics for simulation and prediction.

Dr. Rasha Aly Mohamed was born in Egypt in 1978. She received the B. Sc. degree in Physics and Chemistry, the M.Sc. degree in Fluid Dynamics and Ph.D. degree in Hydromagnetic and Hydrodynamic stability from Faculty of Education Ain Shams University, in 1999, 2006 and 2010, respectively. Dr. Rasha is currently assistant prof. at the Department of Physics, Faculty of Education, Ain Shams University. Her main areas of research interest are Fluid Mechanics, Nano-fluids, Mathematical modelling, Artificial Intelligence and artificial Neural Network Model.

CC BY

Dr. Doaa Mahmoud Habashy was born in Egypt 1980. Dr. Doaa is a researcher in school of Artificial Intelligence. Dr. Doaa received the B. Sc. degree in Physics and Chemistry, the M.Sc. degree in Theoretical Physics and Ph.D. degree in Artificial Neural Network from Faculty of Education, Ain Shams University, in 2001, 2007 and 2011, respectively. Dr. Doaa is a lecturer at the Department of Physics, Faculty of Education, Ain Shams University. Her main areas of research interest are Artificial Intelligence, Neural Network Model and its application in Physics for simulation and prediction

Engy Hany Ali was born in Egypt in 1993. Engy received B.Sc. degree in physics department. Demonstrator at Faculty of Education in physics department. Researcher in Master (applications of Artificial neural networks in physics). Four years of teaching and training experience.

CC BY